What determines the magnitude of carbon cycle-climate feedbacks?

Matthews, H Damon ; Eby, Michael ; Ewen, Tracy ; Friedlingstein, Pierre ; Hawkins, Barbara J

Abstract: Positive feedbacks between climate change and the carbon cycle have the potential to amplify the growth of atmospheric carbon dioxide and accelerate future climate warming. However, both the magnitude of and the processes which drive future carbon cycle- climate feedbacks remain highly uncertain. In this study, we use a coupled climate-carbon model to investigate how the response of vegetation photosynthesis to climate change contributes to the overall strength of carbon cycle-climate feedbacks. We find that the feedback strength is particularly sensitive to the model representation of the photosynthesis-temperature response, with lesser sensitivity to the parameterization of soil moisture and nitrogen availability. In all simulations, large feedbacks are associated with a climatic suppression of terrestrial primary productivity and consequent reduction of terrestrial carbon uptake. This process is particularly evident in the tropics and can explain a large part of the range of carbon cycle-climate feedbacks simulated by different coupled climate-carbon models.

DOI: https://doi.org/10.1029/2006GB002733

What determines the magnitude of carbon cycle-climate feedbacks?

H. Damon Matthews,[1] Michael Eby,[2] Tracy Ewen,[3] Pierre Friedlingstein,[4] and Barbara J. Hawkins[5]

Received 3 April 2006; revised 22 January 2007; accepted 8 March 2007; published 19 May 2007.

[1] Positive feedbacks between climate change and the carbon cycle have the potential to amplify the growth of atmospheric carbon dioxide and accelerate future climate warming. However, both the magnitude of and the processes which drive future carbon cycle-climate feedbacks remain highly uncertain. In this study, we use a coupled climate-carbon model to investigate how the response of vegetation photosynthesis to climate change contributes to the overall strength of carbon cycle-climate feedbacks. We find that the feedback strength is particularly sensitive to the model representation of the photosynthesis-temperature response, with lesser sensitivity to the parameterization of soil moisture and nitrogen availability. In all simulations, large feedbacks are associated with a climatic suppression of terrestrial primary productivity and consequent reduction of terrestrial carbon uptake. This process is particularly evident in the tropics and can explain a large part of the range of carbon cycle-climate feedbacks simulated by different coupled climate-carbon models.

Citation: Matthews, H. D., M. Eby, T. Ewen, P. Friedlingstein, and B. J. Hawkins (2007), What determines the magnitude of carbon cycle-climate feedbacks?, *Global Biogeochem. Cycles*, *21*, GB2012, doi:10.1029/2006GB002733.

1. Introduction

[2] The global carbon cycle is an integral component of the climate system. Levels of atmospheric carbon dioxide (CO_2) are strongly determined by the fluxes of carbon between atmospheric, land and ocean carbon stores. In the context of present anthropogenic emissions of carbon dioxide, the accumulation of CO_2 in the atmosphere is critically dependent on the strength of terrestrial and oceanic carbon sinks. The extent to which current carbon sinks may be affected by climate changes creates the potential for feedbacks between the carbon cycle and climate change. The strength of future carbon cycle-climate feedbacks may be one of the most important uncertainties with respect to determining the magnitude of climate change over the next century.

[3] Numerous model studies have demonstrated the potential for positive carbon cycle feedbacks to operate in the climate system [*Cox et al.*, 2000; *Friedlingstein et al.*, 2001; *Dufresne et al.*, 2002; *Jones et al.*, 2003b; *Zeng et al.*, 2004; *Thompson et al.*, 2004; *Matthews et al.*, 2005b; *Govindasamy et al.*, 2005; *Matthews et al.*, 2005a; *Fung et al.*, 2005]. All of these studies have shown that when climate changes are allowed to affect carbon cycle processes, atmospheric CO_2 growth is amplified owing to weakened terrestrial and oceanic carbon sinks. The strength of the feedback, however, has varied considerably between models, with the amplification of atmospheric CO_2 at the year 2100 ranging from 20 parts per million (ppm) to more than 200 [*Friedlingstein et al.*, 2006]. Both ocean and terrestrial carbon cycles have been found to contribute to the global carbon cycle-climate feedback, though in most cases, the terrestrial component of the feedback has been shown to dominate over the next century. Additionally, most of the variance between models originates from differences in the terrestrial carbon cycle response to climate changes [*Friedlingstein et al.*, 2003, 2006].

[4] A striking feature of the terrestrial carbon cycle response to climate changes is a decrease in soil carbon as a function of climate warming [e.g., *Cox et al.*, 2000]. All models include a positive (exponential) relationship between the rate of soil carbon decomposition (heterotrophic soil respiration) and soil temperature; increasing temperature thus leads to a weakening of the terrestrial carbon sink due to an acceleration of soil carbon release [*Cox et al.*, 2000; *Friedlingstein et al.*, 2003]. As a consequence of this, much research has focused on the response of soil respiration to climate changes as a primary driver of the terrestrial feedback [*Friedlingstein et al.*, 2003; *Jones et al.*, 2003a]. Analysis of this component of the feedback has not, however, been able to reconcile differences in model feedback strengths [*Jones et al.*, 2005;

[1]Department of Geography, Planning and Environment, Concordia University, Montreal, Quebec, Canada.
[2]School of Earth and Ocean Sciences, University of Victoria, Victoria, British Columbia, Canada.
[3]Institute for Atmospheric and Climate Science, ETH Zurich, Zurich, Switzerland.
[4]Institute Pierre Simon Laplace, LSCE, Gif sur Yvette, France.
[5]Centre for Forest Biology, University of Victoria, Victoria, British Columbia, Canada.

0886-6236/07/2006GB002733

Matthews et al., 2005b]. This suggests that while soil respiration is an important component of the terrestrial feedback, it does not on its own explain why different models have produced such divergent results.

[5] In a recent model study using version 2.3 of the University of Victoria Earth System Climate Model (UVic ESCM), *Matthews et al.* [2005b] proposed that an important driver of the terrestrial carbon cycle-climate feedback is the response of vegetation productivity and carbon uptake to climate changes. In particular, the authors argued that large carbon cycle-climate feedbacks require decreases in vegetation productivity due to climate changes, in addition to an acceleration of soil carbon decomposition. In a subsequent study, *Matthews et al.* [2005a] demonstrated that suppression of photosynthesis at high temperatures can greatly amplify the simulated carbon cycle-climate feedback, and that much of the range of model-simulated feedback magnitudes could be explained by differences in terrestrial productivity-climate responses.

[6] In this paper, we expand on the research presented by *Matthews et al.* [2005a] by examining the effect of several environmental limitations on terrestrial carbon uptake in determining the response of the carbon cycle to climate changes. Plants are highly responsive to their local environments, and as such the rate of carbon uptake depends on environmental conditions such as light, nitrogen and water availability, atmospheric carbon dioxide and temperature. Leaf nitrogen, for example, is associated with several physiological stages of photosynthesis, and the rate of photosynthesis is thus strongly affected by nitrogen availability [*Lambers et al.*, 1998]. Water availability is also a key limiting factor for plant growth on a global scale, playing a role in cell expansion, transport and all physiological processes [*Lambers et al.*, 1998]. Furthermore, plant water use can be affected by elevated atmospheric CO_2; in theory, plants are able to gain sufficient carbon with less water loss in a high-CO_2 atmosphere [*Schäfer et al.*, 2002] with the result that CO_2 can affect terrestrial carbon dynamics by both directly stimulating vegetation growth, and also indirectly via plant influence on available soil moisture for soil carbon decomposition. Temperature is also an important limiting factor for photosynthesis due to its effect on the rate of biochemical reactions and enzyme function. The optimum temperature for photosynthesis varies considerably among species (ranging from 5 to 40°C), as does the shape of the photosynthesis-temperature response curve [*Lambers et al.*, 1998; *Kirschbaum*, 2004]. As such, the rate of terrestrial carbon uptake is highly sensitive to the temperature at which photosynthesis occurs.

[7] In this paper, we focus on the response of vegetation productivity to climate changes as a dominant contributor to the net climatic effect on terrestrial carbon uptake in coupled climate-carbon cycle models. In a detailed sensitivity study, we have varied the model representation of the effect of nitrogen limitation, soil moisture and temperature on carbon uptake and storage in vegetation. We present simulated carbon cycle-climate feedbacks for each model configuration, demonstrating the effect of each change to the model on the transient behavior of the climate-carbon cycle system. Finally we apply the feedback analysis of *Friedlingstein et al.* [2003] to the results for each version of the model, and compare the range of model results obtained in this sensitivity study to recently published results from other coupled climate-carbon models [*Friedlingstein et al.*, 2006].

2. Methods

2.1. Model Description

[8] The model used for this study is the University of Victoria Earth System Climate Model (UVic ESCM), version 2.7. The climate component of the model is based on version 2.3 of the UVic ESCM, as described by *Weaver et al.* [2001]. The oceanic component of the UVic ESCM is a general circulation ocean model with horizontal resolution of 1.8 degrees latitude by 3.6 degree longitude, and 19 levels in the vertical. Carbon cycling in the ocean is based on the OCMIP abiotic protocol, with inorganic carbon simulated as a passive tracer in the ocean model [*Ewen et al.*, 2004]. This ocean model is coupled to a dynamic-thermodynamic sea ice model, and a single-layer vertically integrated energy-moisture balance atmosphere [*Weaver et al.*, 2001].

[9] The UVic ESCM has now been coupled to a dynamic vegetation and terrestrial carbon cycle model [*Meissner et al.*, 2003; *Matthews et al.*, 2005b]. The land surface component of the model is a single-soil-layer version of the U. K. Met Office Surface Exchange Scheme (MOSES2 [*Cox et al.*, 1999; *Essery et al.*, 2003]), and is coupled to the TRIFFID dynamic vegetation model (Top-down Representation of Interactive Foliage and Flora Including Dynamics [*Cox*, 2001]). TRIFFID models the spatial distribution of five plant functional types (PFTs): broadleaf trees (BT), needleleaf trees (NT), C_3 grasses (C3), C_4 grasses (C4) and shrubs (SB).

[10] The terrestrial carbon cycle is represented by a coupled photosynthesis-stomatal conductance model based on a biochemical model of photosynthesis for C_3 and C_4 plants [*Collatz et al.*, 1991, 1992]. Carbon uptake through photosynthesis (GPP: gross primary productivity) is calculated within MOSES as a function of ambient CO_2, temperature, soil moisture, light and humidity. Nitrogen availability is prescribed and does not change as a function of changing climatic conditions. Plant growth and maintenance respiration are determined on the basis of environmental conditions, and subtracted from GPP to calculate net carbon uptake or NPP (net primary productivity). NPP is allocated to either leaf, wood or root carbon pools, or to the spread of vegetated area. Vegetation carbon is transferred to the soil through litterfall and then returned to the atmosphere by heterotrophic (soil) respiration, which varies as a function of soil temperature and moisture.

2.2. Model Configurations and Experimental Setup

[11] In this study we have varied the model representation of three key processes in the model which affect terrestrial carbon uptake: (1) the availability of leaf nitrogen, (2) the effect of soil moisture on the rate of leaf turnover, and (3) the effect of temperature as a limiting factor on the rate of photosynthesis. Five versions of the UVic model are presented here, which are listed in Table 1. The base model

Table 1. Model Configurations

Model	Modification From Reference Model Version
NONE	unmodified vegetation parameters
DN	decreased leaf nitrogen availability
DM	inclusion of soil moisture stress on the rate of leaf turnover
DT	decreased temperature control parameters for photosynthesis
ALL	all of the above (DN + DM + DT)

version used for this study (NONE) contains vegetation parameters consistent with the version of the model used in [*Matthews et al.*, 2005b]. Model versions DN, DM and DT have been modified by decreasing nitrogen availability (DN), including the effect of soil moisture stress on the rate of leaf turnover (DM) and decreasing the upper and lower temperature control parameters for photosynthesis (DT). Model version ALL carries all of the modifications of the previous three model versions (DN + DM + DT).

[12] Parameter values for nitrogen availability in the model (specified as the ratio of nitrogen to carbon in leaves) for each plant functional type are listed in Table 2. This specified leaf nitrogen is used in the calculation of the maximum (non-temperature stressed) rate of carboxylation of the photosynthetic enzyme Rubisco ($V_{\max}$: discussed further below), as well as in the model calculation of plant growth and maintenance respiration. In model versions DN and ALL, leaf nitrogen availability is decreased by 25% for all plant functional types, leading to decreased model values for both GPP and NPP (see Table 3). This change is well within the natural range of leaf nitrogen concentrations, which can vary from.0068 to.062 kg N/kg C depending on species, site and environmental conditions [*Reich et al.*, 1997, 1999].

[13] Soil moisture affects vegetation processes in the carbon cycle model in several ways. There is a direct impact on photosynthesis, whereby stomata close if soil moisture decreases beyond the vegetation wilting point. Where there is sufficient soil moisture for photosynthesis to occur, the net rate of photosynthesis increases linearly with soil moisture up to a saturation soil moisture level, above which vegetation is no longer limited by soil moisture availability. Soil moisture also affects the rate of plant and soil respiration, which in turn determine the net terrestrial carbon uptake. Furthermore, the model contains a parameterization for a direct effect of soil moisture on litterfall or the rate of leaf turnover. However, in previous studies using the UVic ESCM coupled to MOSES and TRIFFID, this parameterization was not activated in the model [e.g., *Meissner et al.*, 2003; *Matthews et al.*, 2005b].

Table 3. Simulated Equilibrium Terrestrial Carbon Fluxes and Stores[a]

Model	GPP, GtC/yr	NPP, GtC/yr	CV, GtC	CS, GtC	T, K
NONE	189	85	1204	1371	287.65
DN	158	74	1045	1144	287.15
DM	159	73	745	1140	286.55
DT	185	86	1088	1444	287.5
ALL	134	64	571	1059	286.15

[a]Fluxes are gross primary productivity (GPP) and net primary productivity (NPP). Stores are vegetation carbon (CV) and soil carbon (CS). Globally averaged surface air temperature is also listed for each model (T).

[14] The leaf turnover rate in the model (ΔL) is calculated as

$$\Delta L = \Delta L_{\min} \cdot F(T) \cdot F(M), \tag{1}$$

where $\Delta L_{\min}$ is the minimum rate of leaf turnover (set to 0.25 for all PFTs) and $F(T)$ and $F(M)$ are a PFT-dependent temperature (T) and fractional soil moisture availability (M) effect on the leaf turnover rate. In model version DM, we have introduced the formula for $F(M)$,

$$F(M) = 1.0 + k(M_{crit} - M), \tag{2}$$

for cases where soil moisture (M) is less than a specified critical soil moisture level (M_{crit}). In this equation, k is a constant representing the rate of change of the leaf turnover rate with soil moisture. Specified values of M_{crit} are shown in Table 2. For model versions NONE, DN, and DT, $F(M)$ is set to 1.0 for all plant functional types (since $M_{crit} = 0.0$): equation (2) is only used to increase the rate of leaf turnover in model versions DM and ALL.

[15] In many terrestrial carbon cycle models, as well as for most plant species, photosynthesis has an approximate Gaussian dependence on leaf temperature [*Cox et al.*, 1999;

Table 2. Description of Model Configurations and Modified Parameter Values

	Leaf Nitrogen, kg N/kg C					Critical M for Leaf Drop				
Model	BL	NL	C3	C4	SB	BL	NL	C3	C4	SB
NONE	0.04	0.03	0.06	0.03	0.03	0.0	0.0	0.0	0.0	0.0
DN	0.032	0.024	0.048	0.024	0.024	0.0	0.0	0.0	0.0	0.0
DM	0.04	0.03	0.06	0.03	0.03	0.90	0.65	0.15	0.05	0.65
DT	0.04	0.03	0.06	0.03	0.03	0.0	0.0	0.0	0.0	0.0
ALL	0.032	0.024	0.048	0.024	0.024	0.90	0.65	0.15	0.05	0.65
	Upper T Limit					Lower T Limit				
	BL	NL	C3	C4	SB	BL	NL	C3	C4	SB
NONE	36.0	31.0	36.0	45.0	36.0	0.0	−5.0	0.0	13.0	0.0
DN	36.0	31.0	36.0	45.0	36.0	0.0	−5.0	0.0	13.0	0.0
DM	36.0	31.0	36.0	45.0	36.0	0.0	−5.0	0.0	13.0	0.0
DT	31.0	26.0	31.0	40.0	31.0	−5.0	−15.0[a]	−5.0	8.0	−5.0
ALL	31.0	26.0	31.0	40.0	31.0	−5.0	−15.0	−5.0	8.0	−5.0

[a]T_{low} for needleleaf trees was decreased by 10°C relative to NONE so as to improve the simulation of northern boreal forests.

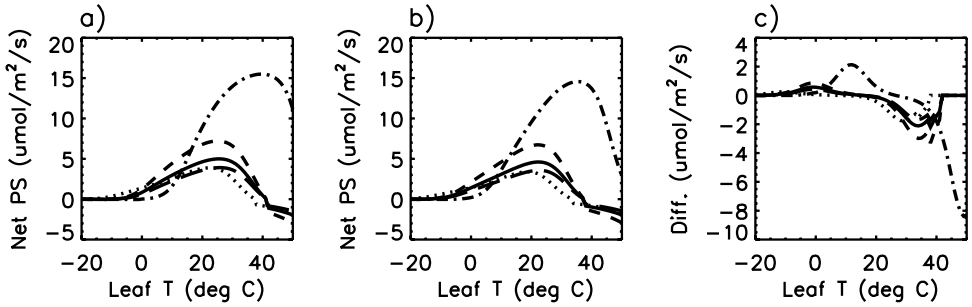

Figure 1. Dependence of net photosynthesis (PS) on leaf temperature (T) (for a specific location with specified soil moisture) for the five PFTs in the model: BL (solid line), NL (dotted line), C3 (short-dashed line), C4 (dash-dotted line) and SB (long-dashed line). (a) The effect of parameters used in NONE, DN and DM, and (b) the effect of parameters used in DT and ALL, in which T_{up} and T_{low} were both decreased by 5°C. (c) The difference between Figures 1 and 1b.

Adams et al., 2004; *Medlyn et al.*, 2002b]. This relationship is shown for the five TRIFFID PFTs in Figure 1. To modify the temperature dependence of photosynthesis, we have decreased the model parameters T_{up} and T_{low}, which are used in the calculation of the temperature limited maximum rate of carboxylation of the photosynthetic enzyme Rubisco (V_m),

$$V_m = \frac{V_{\max} f_T(2.0)}{\left[1+\exp\{0.3(T_c - T_{up})\}\right]\left[1+\exp\{0.3(T_{low} - T_c)\}\right]}. \quad (3)$$

Here T_{up} and T_{low} are the upper and lower temperature constraints on photosynthesis, T_c is the leaf temperature, $V_{\max}$ is a nitrogen-limited (non-temperature stressed) maximum carboxylation rate, and f_T is a standard "Q_{10}" temperature dependence with Q_{10} = 2.0. V_m is used to calculate the gross canopy photosynthesis as limited by Rubisco, available light or the transport of photosynthetic products, which then goes into the calculation of GPP and NPP [*Cox et al.*, 1999]. In model versions DT and ALL (Figure 1b), T_{up} and T_{low} are both decreased by 5°C for all PFTs relative to NONE, DM and DN (Figure 1a); this shifts the photosynthesis-temperature curve toward colder values and thus increases (decreases) the temperature stress on photosynthesis at high (low) temperatures (Figure 1c).

[16] Modification of these vegetation parameters, as listed in Table 2, had large effects on the simulated pre-industrial vegetation distribution. Values for GPP, NPP, vegetation (CV) and soil (CS) carbon for each model version are shown in Table 3. The changes made in each model version (DN, DM and DT) all served to increase climatic limitations on terrestrial carbon uptake and storage, as reflected in decreases in simulated GPP, NPP and CV. It is clear that the combination of all modifications (model version ALL) resulted in the closest correspondence with observational estimates of terrestrial carbon fluxes and stores (e.g., 52.9 to 62.6 GtC/yr for NPP; 650 GtC for CV; 1550 GtC for CS [*Saugier et al.*, 2001; *Prentice et al.*, 2001]), as well as spatial distributions of plant functional types [*Loveland and Belward*, 1997] (not shown). It is also clear that the other four model versions (NONE, DN, DM and DT) do not well reflect observational estimates. We argue, however, that errors in pre-industrial vegetation distributions are less important than direct effect of parameter modifications on the transient response of different model versions. Furthermore, the intent of this paper is not to determine what constitutes the "best" version of the UVic model (the reader is referred to *Meissner et al.* [2003] and *Matthews et al.* [2005b] for a more detailed validation of the UVic ESCM against observations), but rather to explore how the above changes to vegetation parameters in the model affect the transient behavior of the carbon cycle in the context of anthropogenic climate change.

[17] For each version of the model, the UVic ESCM was spun up to equilibrium (~2000 years), and then transient simulations were performed from the year 1750 to 2100. Simulations were forced by historical anthropogenic carbon emissions from fossil fuels and land-use change until 2000 [*Marland et al.*, 2002; *Houghton*, 2003] and then by SRES A2 scenario emissions from 2000 to 2100 [*Nakićenović et al.*, 2000]. Changes in the spatial extent of anthropogenic land-use were not included in these simulations. To isolate the effect of carbon cycle-climate feedbacks, two transient simulations were carried out: (1) a coupled simulation in which both CO_2 increases and associated climate changes were calculated and coupled with the carbon cycle and (2) an uncoupled simulation in which CO_2 increases did not exert any radiative forcing to climate, and the carbon cycle thus responded to increased CO_2 in the context of a constant pre-industrial climate. Differences in simulated atmospheric CO_2 between coupled and uncoupled simulations represent the magnitude of carbon cycle-climate feedbacks in each model version.

3. Results

3.1. Global Carbon Cycle Changes and Feedbacks

[18] Results from coupled and uncoupled runs for the 5 model versions are tabulated in Table 4. Shown here are modeled changes in surface air temperature, carbon pools and terrestrial carbon fluxes from 1750 to 2100 for both coupled and uncoupled model simulations, as well as the differences between coupled and uncoupled model runs at 2100. Global temperature changes in the coupled runs,

Table 4. Coupled and Uncoupled Model Results at 2100 for the Five Model Versions[a]

Model	ΔT, °C	CO_2, ppm	ΔCV, GtC	ΔCS, GtC	ΔDIC, GtC	ΔGPP, GtC/yr	ΔNPP, GtC/yr	ΔR_H, GtC/yr	Δ τ, years
					Coupled (Uncoupled) Run				
NONE	3.1 (0.2)	770 (681)	392 (371)	374 (550)	510 (540)	117.4 (99.2)	70.5 (69.3)	64.9 (61.1)	−4.4 (−1.9)
DN	3.3 (0.2)	798 (718)	377 (353)	314 (454)	526 (576)	101.7 (82.5)	61.5 (58.5)	56.6 (51.8)	−4.3 (−1.8)
DM	3.5 (0.2)	840 (736)	293 (282)	275 (470)	561 (594)	102.0 (85.2)	58.0 (56.0)	54.0 (49.4)	−4.5 (−2.5)
DT	3.4 (0.2)	874 (715)	332 (376)	154 (438)	571 (575)	80.4 (77.8)	42.0 (51.9)	40.7 (44.9)	−4.2 (−2.4)
ALL	3.9 (0.2)	926 (780)	238 (284)	110 (346)	603 (625)	64.7 (61.2)	33.9 (39.2)	32.0 (34.1)	−4.4 (−2.2)
					Difference: Coupled−Uncoupled Runs				
NONE	2.9	89	20.9	−176	−30.1	18.2	1.2	3.8	−1.5
DN	3.1	80	24.3	−140	−50.0	18.2	3.0	4.8	−1.5
DM	3.3	104	10.71	−195	−32.6	16.8	2.0	4.6	−2.0
DT	3.2	159	−43.3	−283	−4.1	2.6	−9.9	−4.2	−1.8
ALL	3.7	146	−45.8	−236	−22.3	3.5	−6.3	−1.9	−2.2

[a]Listed here are surface air temperature increase (T), atmospheric CO_2 and changes in vegetation carbon (CV), soil carbon (CS), ocean dissolved inorganic carbon (DIC), gross primary productivity (GPP), net primary productivity (NPP), soil respiration (R_H), and soil turnover time (τ). Differences at 2100 between coupled and uncoupled runs are shown in the lower half of the table.

listed in the first column, largely reflect differences in simulated atmospheric CO_2 between the five model versions, though there are also small differences in the climate response to CO_2 forcing due to differences in pre-industrial climatology, as well as the dynamics of terrestrial vegetation over the course of the model runs. The small warming seen in the uncoupled simulations results from the effect of CO_2 fertilization of terrestrial vegetation and associated dynamic vegetation feedbacks to climate.

[19] There is a large range in predicted year 2100 CO_2 in the coupled runs, from 770 (NONE) to 926 ppm (ALL) (Table 4 and Figure 2a). Part of this difference can be attributed to differing biospheric response to CO_2 alone, as can be seen in differences in the predicted CO_2 in the uncoupled runs. There are also large differences in the response of the carbon cycle to climate change; the effect of carbon cycle-climate feedbacks on atmospheric CO_2 for the five model versions are shown in Figure 2b as the CO_2 difference between coupled and uncoupled runs. The smallest feedback is seen in model DN, which simulated an additional 80 ppm CO_2 at 2100; the largest feedback is seen in DT, which led to an increased year 2100 CO_2 of 159 ppm.

[20] Changes in vegetation and soil carbon for the five model versions are shown in Figures 2c–2f. In all runs, vegetation carbon increased throughout the model simulation (Figure 2c); the largest increase in vegetation carbon was simulated by NONE (+392 GtC) and the smallest by ALL (+238 GtC). When the difference in vegetation carbon between coupled and uncoupled runs is plotted (Figure 2d), a distinct grouping of models emerges. In runs NONE, DN and DM, vegetation carbon was larger in the coupled run than in the uncoupled runs; this can be explained by a higher atmospheric CO_2 in the coupled run and consequent stronger fertilization of vegetation growth and accumulation of vegetation carbon. In DT and ALL, however, vegetation carbon storage was lower in the coupled than the uncoupled run; in these cases, climate changes had a negative impact on vegetation carbon storage, which outweighed stronger CO_2 fertilization in the coupled run. In all cases, carbon cycle-climate feedbacks reflected the extent to which vegetation carbon storage was suppressed by climate changes; larger feedbacks are associated with a negative impact of climate change on vegetation carbon uptake.

[21] This grouping of models is also apparent when looking at soil carbon changes. Larger feedbacks are associated with lower accumulation of soil carbon in the coupled runs, and in the case of DT and ALL, a slight decrease in global soil carbon toward the end of the simulation (Figure 2e). Also, larger soil carbon differences between coupled and uncoupled runs are associated with larger feedbacks (Figure 2f). It is important to emphasize, however, that these differences did not emerge from model differences in the representation of soil carbon release, as soil respiration was parameterized identically in all model versions. Instead, differences soil carbon emerged from differences in vegetation carbon accumulation and the transfer of carbon from vegetation to soil carbon pools via litterfall. In runs with less vegetation carbon accumulation, less carbon was transferred to the soil carbon pool, and this resulted in less soil carbon storage.

[22] In Figure 2g, changes in ocean dissolved inorganic carbon (DIC) primarily reflect atmospheric CO_2 concentrations in the coupled runs. The coupled-uncoupled DIC difference for each model run (Figure 2h) includes the effect of differences in atmospheric CO_2 (leading to increased uptake) plus the influence of positive climate feedbacks (changes in sea surface temperatures, sea ice and circulation). In Figure 2h, the difference in DIC initially increased slightly for all models until year 2000, as higher atmospheric CO_2 had a larger effect on uptake than increasing ocean temperature and other feedbacks. After this point, positive feedbacks dominated (particularly in DN and NONE, which had the lowest CO_2 concentrations in the coupled runs) and the coupled-uncoupled DIC difference became negative. In the other three model versions, the effect of higher CO_2 in the coupled run dominated for somewhat longer, with DT exhibiting the largest increase in atmospheric CO_2 and consequently showing the smallest difference in DIC between the coupled and uncoupled model runs at the end of the simulation. Differences in ocean feedback strength between models versions, however, were not large relative to differences in the terrestrial feedback, which is not surprising since ocean differences arose solely from differences in climate that were initiated by terrestrial vegetation

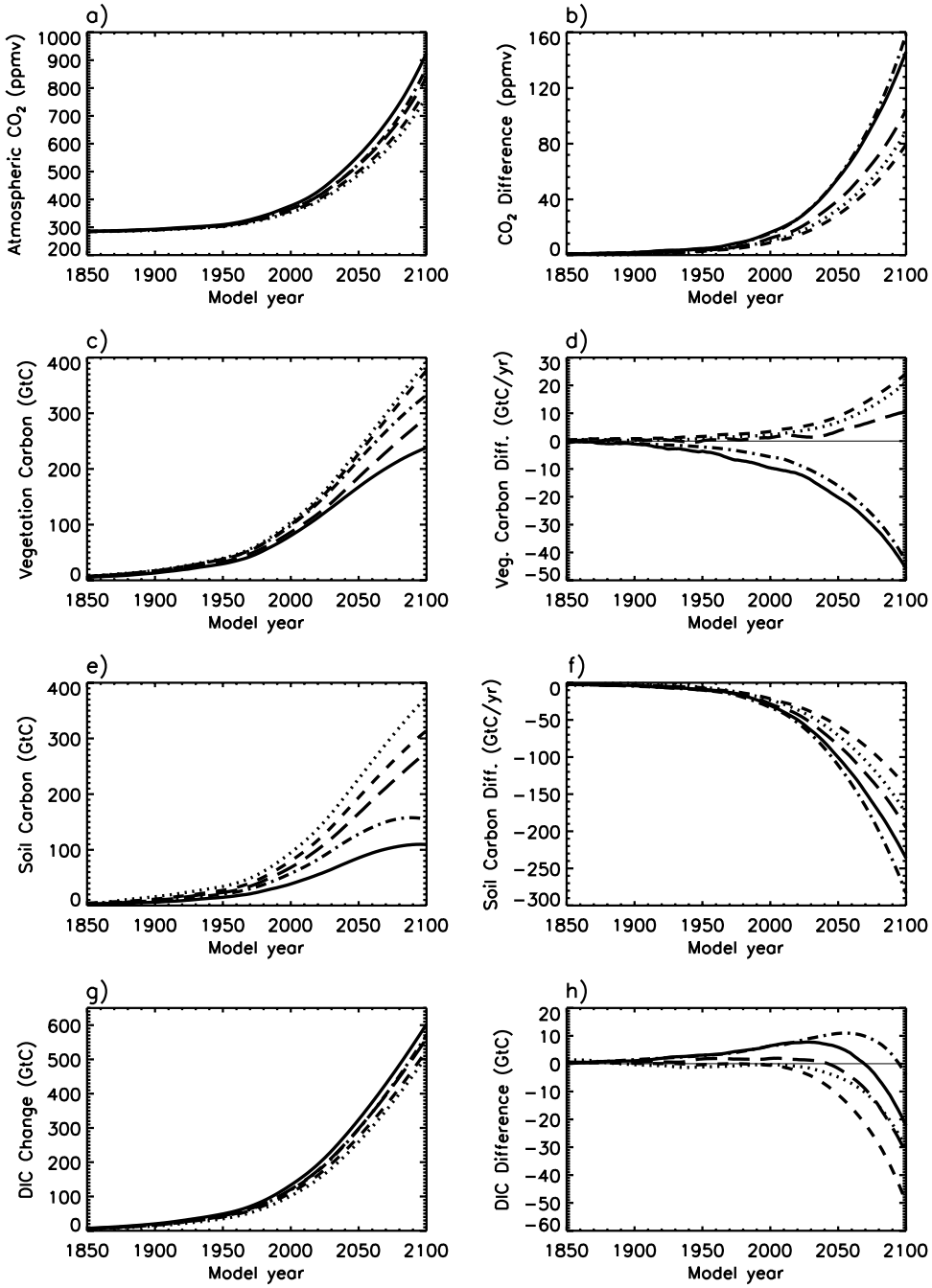

Figure 2. Modeled changes in atmospheric, terrestrial and ocean carbon pools from 1850 to 2100. (a) Modeled atmospheric CO_2 in the coupled runs; (b) CO_2 difference between coupled and uncoupled runs; (c, e, g) vegetation/soil/ocean carbon increases in the coupled runs; and (b, f, h) vegetation/soil/ocean carbon difference between coupled and uncoupled runs. NONE, dotted line; DN, short-dashed line; DM, long-dashed line; DT, dash-dotted line; ALL, solid line.

differences, and not from any modifications to ocean carbon cycle model formulations.

[23] The terrestrial carbon cycle differences apparent in Figure 2 can also be seen in the behavior of terrestrial carbon fluxes (GPP, NPP and soil respiration) in the five models, as plotted in Figure 3. In Table 4, GPP can be seen to have increased in all models, ranging from an increase of 65 GtC in ALL to 117 GtC in NONE for the coupled runs. GPP increases in the uncoupled runs were all smaller, on account of lower atmospheric CO_2 (from 61.2 in ALL to 99 in NONE). The difference between coupled and uncoupled simulations (shown in Figure 3a) reveals the same grouping of models as was seen for vegetation and soil carbon; models DT and ALL show a large climatic suppression of

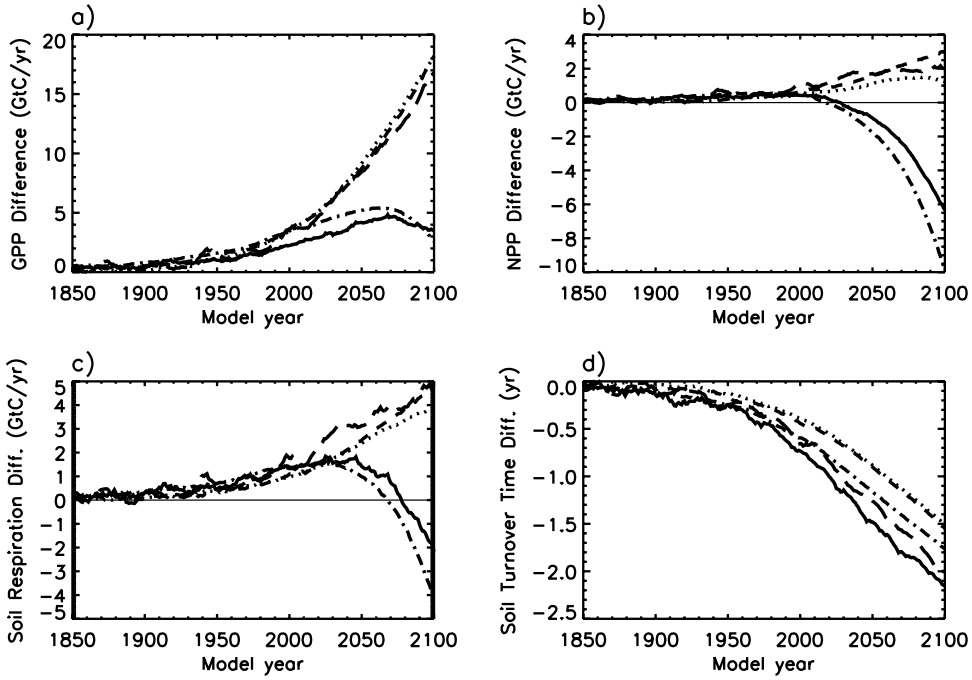

Figure 3. Modeled difference in terrestrial carbon fluxes and turnover times from 1850 to 2100. (a, b) GPP/NPP difference between coupled and uncoupled runs; (c, d) as for Figures 3a and 3b for soil respiration and soil carbon turnover time. NONE, dotted line; DN, short-dashed line; DM, long-dashed line; DT, dash-dotted line; ALL, solid line.

GPP, whereas in models DN, DM and NONE, GPP was much less affected by climate changes. When NPP changes are plotted in a similar manner (Figure 3b), the same pattern emerges, though in this case, the differences in NPP between coupled and uncoupled runs are either positive (higher NPP in the coupled runs, as for NONE, DN and DM) or negative (lower NPP in the coupled runs, as in DT and ALL). Again, larger carbon cycle-climate feedbacks are associated with climate suppression of photosynthesis and consequent vegetation carbon uptake and storage.

[24] The importance of GPP and NPP changes in determining the magnitude of carbon cycle-climate feedbacks is also apparent in the response of soil respiration in the five model versions. In all models, soil respiration increased throughout the simulation (Table 4); in the uncoupled runs, soil respiration changes can be explained primarily by changes in the soil carbon pool, as soil temperature did not change in these runs. In the coupled runs, soil respiration was affected by changes in climate; however, these runs also experienced changes in soil carbon input from vegetation, and hence the size of the soil carbon pool over time varied considerably between model versions. The dependence of the rate of soil respiration on vegetation carbon inputs is clear in the plot of differences between coupled and uncoupled runs (Figure 3c). In models DT and ALL, soil respiration was actually decreased in the coupled run relative to the uncoupled run as a consequence of decreased vegetation carbon input, despite increased soil respiration from temperature increases in the coupled run.

[25] The behavior of soil carbon processes in these runs can be further analyzed by examining changes in soil turnover time (τ, in years), defined here as the ratio of total soil carbon (CS) to the rate of soil respiration (R_H),

$$\tau = \frac{CS}{R_H}. \tag{4}$$

The change in soil turnover time in the five models is listed in the final column of Table 4. In all models, τ decreased throughout the simulation; in the coupled runs, this represents an increase in soil respiration relative to total soil carbon, such as would be caused by increased soil temperature. Surprisingly, τ also decreased in the uncoupled simulations, in which soil temperature changes were negligible. These simulations did, however, produce a change in soil moisture, since at higher CO_2, vegetation uses water more efficiently; as a result, evaporation was lower and soil moisture increased. The decreased turnover times in these runs resulted from increased soil moisture and consequent increased soil respiration relative to total soil carbon in areas where soil respiration was limited by soil moisture.

[26] Differences in soil turnover time between coupled and uncoupled model runs represent the contribution of accelerated soil respiration due to climate changes to the total carbon cycle-climate feedback. As can be seen in Figure 3d, all model versions showed an acceleration of soil respiration due to climate changes (decreased τ). Differences between model versions, however, are not large. Furthermore, most of the difference arises from differences in the uncoupled runs, rather than the coupled runs (Table 4). This result suggests that model differences

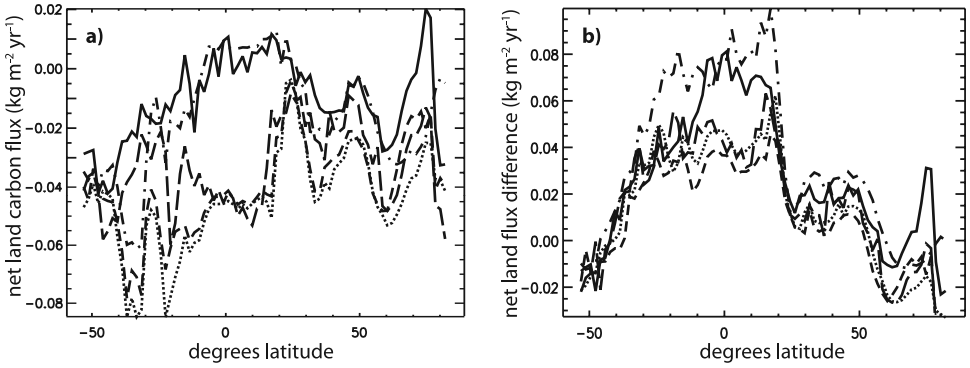

Figure 4. Zonally averaged (a) net terrestrial carbon flux at 2100 in the coupled run (positive denotes carbon source; negative denotes carbon sink) and (b) net terrestrial carbon flux difference between coupled and uncoupled runs at 2100 (positive denotes increased carbon source/decreased carbon sink). NONE, dotted line; DN, short-dashed line; DM, long-dashed line; DT, dash-dotted line; ALL, solid line.

in how soil respiration responded to climate changes are better explained by soil moisture than temperature effects on τ.

3.2. Regional Carbon Cycle Changes

[27] The UVic ESCM is a spatially explicit model, and as such it is informative to look at the latitudinal distribution of the global terrestrial carbon cycle changes discussed in the previous section. The net land flux to the atmosphere in the coupled run (the difference between R_H and NPP at 2100) is shown for the five model versions in Figure 4a. As can be seen here, model runs NONE, DM and DN showed a terrestrial carbon sink at all latitudes (shown here as a negative net carbon flux, representing a flux of carbon out of the atmosphere). Particularly notable in these runs is a strong tropical carbon sink that persisted through to the year 2100. This was not the case for runs ALL and DT, which differed from the other three runs primarily in the tropics: In these two runs, latitudes between about 10°S and 30°N represented a net terrestrial carbon source to the atmosphere at the year 2100. This is a direct reflection of the increased heat stress affecting photosynthesis in these model versions, with a dominant effect occurring in tropical regions.

[28] The contribution of these between-model differences in NEP to the net carbon cycle-climate feedback can be seen in Figure 4b, which shows the difference in the year 2100 net terrestrial carbon flux to the atmosphere between coupled and uncoupled runs. For all model configurations, the net carbon flux difference is predominantly positive, reflecting the effect of climate changes leading to reduced terrestrial carbon uptake in the coupled run relative to the uncoupled run. It is in the tropics, however, that the differences between model configurations is most apparent, with models ALL and DT showing a notably larger change in net carbon uptake due to the suppression of NPP at high temperatures in the tropics. It is interesting to note here that at high Northern and Southern latitudes the terrestrial carbon cycle actually represents a negative feedback to climate, as terrestrial carbon uptake at high latitudes is stronger in the coupled run on account of climate warming. This effect is small, however, relative to positive feedbacks in the tropics and midlatitudes.

3.3. Feedback Analysis

[29] In this section, we apply the feedback analysis of *Friedlingstein et al.* [2003] to results from the five model versions. This analysis serves to separate the relative contribution of different components of the carbon cycle to the overall feedback, as well as to isolate the effect of climate changes from the opposing effect of higher CO_2 in the coupled runs. This is done by characterizing carbon cycle changes in terms of beta (β) and gamma (γ) values. β-values are derived from the uncoupled run only, and represent the carbon cycle sensitivity to atmospheric CO_2 increases (in the absence of climate change),

$$\Delta C^u = \beta \Delta C_A^u. \tag{5}$$

Here ΔC^u is the uncoupled-run change in either land or ocean carbon storage (in GtC) and ΔC_A^u is the change in atmospheric CO_2 (in ppm) in the uncoupled run. The ratio of land carbon change (ΔC_L^u) to ΔC_A^u gives a value of β for land only (β_L in GtC/ppm).

[30] The γ-values represent the carbon cycle sensitivity to climate changes,

$$\Delta C^{clim} = \gamma \Delta T^c. \tag{6}$$

Here ΔT^c is the globally averaged temperature change in the coupled run, and ΔC^{clim} is the change in (either land or ocean) carbon storage due to climate changes. Since ΔC^c (the change in carbon storage in the coupled run) is influenced by both climate change and atmospheric CO_2 increases, ΔC^c must be corrected for higher CO_2 in the coupled run to calculate the change in carbon storage due to climate changes alone (ΔC^{clim}),

$$\Delta C^{clim} = (\Delta C^c - \Delta C^u) - \beta\left(\Delta C_A^c - \Delta C_A^u\right). \tag{7}$$

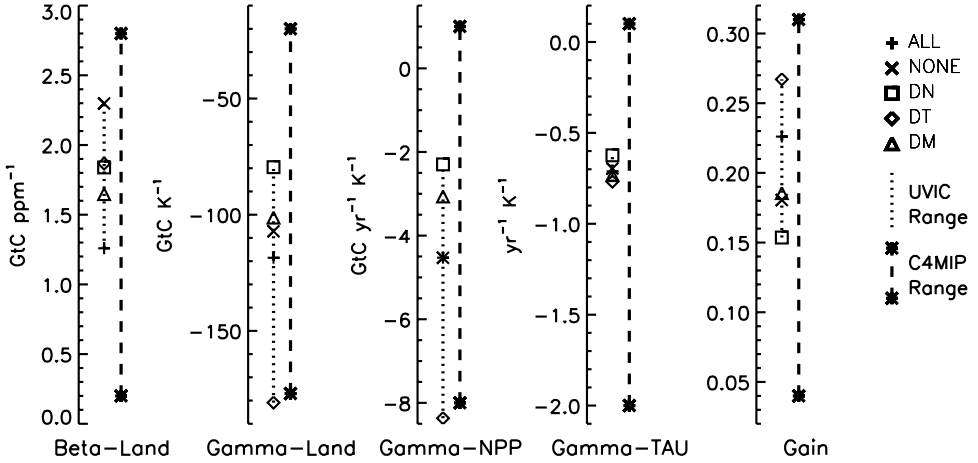

Figure 5. Feedback analysis parameters for the five UVic model versions, compared to the C4MIP inter-model range. Parameters shown (from left to right) are beta-land (β_L) and gamma-land (γ_L) (both with units of GtC/ppm), gamma-NPP (γ_{NPP}) and gamma_TAU ($\gamma\tau$) (units of GtC/yr/K), and gain (g: unitless). For each parameter, symbols on the dotted line show the range covered by the five UVic model versions; the adjacent dashed line shows the C4MIP intermodel parameter range from *Friedlingstein et al.* [2006], with upper and lower symbols indicating the maximum and minimum values.

Consequently, γ_L, calculated as: $\gamma_L = \Delta C_L^{clim}/\Delta T^c$, represents the terrestrial carbon cycle contribution to positive carbon cycle-climate feedbacks (in GtC/K).

[31] *Friedlingstein et al.* [2003] also defined the gain of the carbon cycle-climate feedback (g) as

$$\Delta C_A^c = 1/(1-g)\Delta C_A^u, \tag{8}$$

where a g of zero represents no feedback, and $0 < g < 1$ represents the effect of positive carbon cycle-climate feedbacks on atmospheric CO_2. As shown in *Friedlingstein et al.* [2003, 2006], g can also be expressed as a function of β and γ parameters,

$$g = -\alpha(\gamma_L + \gamma_O)/(1 + \beta_L + \beta_O). \tag{9}$$

Here subscripts L and O indicate β and γ parameters for land and ocean, respectively, and α is an additional parameter representing the transient climate warming response to CO_2 (in K/ppm).

[32] Values of g, α, β_L, β_O, γ_L, and γ_O from 12 different coupled climate-carbon models have recently been published as part of the Coupled Climate Carbon Cycle Intercomparison Project (C4MIP) [*Friedlingstein et al.*, 2006]. In this section, we apply this feedback analysis specifically to the terrestrial carbon cycle, and compare parameter values of g, β and γ from the five UVic model versions used in this paper to published results from the range of C4MIP models.

[33] Result of this analysis are shown in Figure 5. For each parameter, each UVic model version is plotted by a symbol as indicated in the Figure 5 legend, with the UVic model range indicated by a dotted line. The adjacent dashed line indicates the range of C4MIP models, with maximum and minimum vales indicated by the upper and lower symbols. In addition to values of β_L, γ_L and g (as defined by equations (5), (6) and (8) above), Figure 5 also shows values of γ_{NPP} and $\gamma\tau$, corresponding to the γ values for net primary productivity (NPP) and soil turnover time (τ), respectively. These were calculated by the same method as γ_L, but using values for ΔNPP and $\Delta\tau$ in place of ΔC_L in equations (6) and (7), along with their respective β_{NPP} and $\beta\tau$ values.

[34] From the parameter ranges plotted in Figure 5, is it clear first that the five UVic model versions do differ considerably with respect to their β_L values. This difference largely reflects different starting vegetation distributions, with model versions that simulated more pre-industrial land carbon storage, also exhibiting a greater capacity to take up anthropogenic carbon (higher β_L). Differences in β_L do affect the strength of carbon cycle-climate feedbacks, as a decreased β_L results in higher atmospheric CO_2 which generates more climate change and hence a larger impact on the carbon cycle (see also equation (9)). This is likely an important factor in the increased feedback strength in the DM model run, as of the three perturbed runs (DT, DN and DM), DM showed the largest decrease in β_L relative to NONE. However, differences in β_L are not the most important contributor to overall differences in feedback strength between the model versions. For example, DN also showed a decrease in β_L relative to NONE, though as shown in Figure 2b, the DN model feedback was smaller than NONE. Furthermore, DT (largest feedback), did not have the smallest β_L, and in fact had a very similar β_L to DN (smallest feedback).

[35] More significant, is the large range between model versions in γ_L values. As would be expected, DT shows the largest (most negative) γ_L, corresponding with a large negative effect of climate warming on photosynthesis and consequent terrestrial carbon uptake. It is interesting to note

here, however, that there is no additivity in the γ_L values of the perturbed model versions. In particular, the difference in γ_L between ALL and NONE does not reflect the sum of the individual differences between DN, DM, DT and NONE, respectively. This speaks to interesting nonlinearities in the terrestrial biosphere response to climate change, which would bear further research.

[36] Differences in γ_L between model versions can be related directly to differences in γ_{NPP} and γ_τ. Land carbon changes (ΔC_L) can be calculated as the time-integrated difference between NPP and R_H. It follows that γ_L reflects the time-integrated difference between γ_{NPP} and γ_{RH}. However, as discussed in the previous section, changes in R_H are not independent of changes in NPP: as such, γ_τ is a better reflection of the soil respiration contribution to terrestrial carbon cycle-climate feedbacks. Hence γ_L can be approximated as $\gamma_L = \Delta time\ (\gamma_{NPP} - \gamma_\tau \Delta CS)$. Since γ_τ differences between UVic model versions are small, it follows that the majority of the range in γ_L can be attributed differences in γ_{NPP}. In other words, differences in the NPP response to climate changes control the extent by which the terrestrial carbon cycle is affected by climate changes.

[37] These β and γ parameter ranges can used to explain the range in g between the five UVic model versions. As shown by *Friedlingstein et al.* [2003], the partial derivatives of g (from equation (9)) with respect to β_L and γ_L can be expressed as

$$\frac{\partial g}{\partial \beta_L} = \alpha(\gamma_L + \gamma_O)/(1 + \beta_L + \beta_O)^2 \tag{10}$$

$$\frac{\partial g}{\partial \gamma_L} = -\alpha/(1 + \beta_L + \beta_O). \tag{11}$$

Using average values of α, β_O and γ_O, we calculate that the γ_L range between UVic model versions would by itself result in a range of 0.12 in g. Similarly, the range in β_L between model versions represents a range of -0.04 in g. The actual range in g between model versions is 0.11, indicating that the effect of γ_L differences between model versions on g is reduced to some extent by differences in β_L, as well as by smaller differences in α, β_O and γ_O. We can conclude that the range of g between model versions is dominated by differences in γ_L, which are themselves dominated by differences in γ_{NPP}. This range of g between UVic model versions covers 42% of the full C4MIP g range.

[38] Applying a similar calculation to the range of C4MIP models, we estimate that the C4MIP range of γ_L and β_L would by themselves result in g ranges of 0.21 and -0.08, respectively (the actual range g values between C4MIP models is 0.27). While this calculation is approximate (recognizing that α, β and γ parameter values are not independent, nor is there any evidence that their individual effects on g combine linearly), it does support the claim made by *Friedlingstein et al.* [2006] that variation in γ_L between model values is the dominant contributor to the large intermodel range in g. On the basis of the UVic model parameter ranges presented above, we argue that intermodel differences in how NPP responds to climate changes (as reflected by the C4MIP γ_{NPP} range) could account for up to about half of the intermodel range in the carbon cycle-climate feedback gain.

4. Discussion

[39] In this paper, we have investigated the response of the carbon cycle to climate changes in five versions of an intermediate complexity coupled climate-carbon cycle model. To explore the model sensitivity to vegetation parameters, we have modified the extent of nitrogen limitation (DN), the effect of soil moisture on rates of leaf turnover (DM) and the temperature limitation of photosynthesis (DT). The feedback between climate and the carbon cycle in each model version is analyzed, and compared to an unperturbed model version (NONE) and a model version with all modifications (ALL).

[40] The sensitivity of the carbon cycle-climate feedback in the model to changes in model parameters varied considerably between model versions. In DN, increasing nitrogen limitation actually decreased the net carbon cycle-climate feedback. Since nitrogen affects both the rate of photosynthesis and also the rate of plant respiration in the model, this change indicates that increased nitrogen limitation on balance decreased the response of plant respiration to climate changes more than the response of photosynthesis. The net effect on the carbon cycle-climate feedback was small, indicating that this feedback is not very sensitive to the representation of nitrogen limitation in the model. It is important to emphasize here, however, that the nitrogen limitation imposed here does not represent a decreased availability of nitrogen in the model as a function of time. In fact, since the nitrogen:carbon ratio in the model is fixed, as vegetation carbon increased, nitrogen also increased, implying an increasing supply of nitrogen under future climate change. This does not necessarily reflect how the nitrogen cycle will behave in the future [e.g., *Hungate et al.*, 2003] and as such does not invalidate the possibility of strong interactions and feedbacks between nitrogen and carbon cycles in response to future climate change.

[41] In model version DM, the carbon cycle-climate feedback did increase notably from model version NONE. This case is interesting, however, as there was no evidence of increased soil moisture limitation on photosynthesis over the course of this model run, which could explain an increased carbon cycle-climate feedback. For example, γ_{NPP} for DM was actually smaller than γ_{NPP} for NONE, which would imply a smaller carbon cycle-climate feedback were climate change effects on NPP to be directly responsible. As such, the amplification of the carbon cycle feedback in this run likely resulted from changes in the soil moisture regime as a function of both climate and CO_2 effects on vegetation, which led to decreases in the soil turnover time in this run relative to NONE. Several experimental studies have found soil carbon decomposition rates to be limited by available soil moisture [e.g., *Aerts*, 2006]; to date, modeling studies have only hinted at significant future soil moisture-carbon cycle interaction [e.g., *Fung et al.*, 2005], and as such this represents an open question which warrants future investigation. It is also worth noting

that there may be important interactions between nitrogen availability and leaf turnover rates that were not captured here; for example, leaves with short lifespans tend to have more nitrogen than longer-life leaves [*Wright et al.*, 2004]. Further model improvement, particularly with respect to the representation of nitrogen, would be required to address the importance of such interactions under changing climatic conditions.

[42] By far the largest impact of vegetation parameters on the carbon cycle-climate feedback occurred in model version DT. In this case the mechanism for amplification of the carbon cycle-climate feedback is clear: increasing the temperature stress on photosynthesis in the model required plants to photosynthesize at increasingly suboptimal temperatures under future climate warming. The consequent large negative effect of climate changes on NPP led to greatly reduced terrestrial carbon uptake and amplification of the terrestrial carbon cycle-climate feedback. As noted in the introduction, there is a high degree of interspecies variability in the specific shape of the photosynthetic-temperature response curve, as well as the optimum temperature for photosynthesis; in real environments, the temperature constraint on photosynthesis is further affected by CO_2 concentration, water and nitrogen availability [*Kirschbaum*, 2004], and many plants also exhibit an ability to acclimate to changing temperatures, both seasonally and over the longer term [*Berry and Björkman*, 1980; *Medlyn et al.*, 2002a, 2002b]. Given the poor observational constraints on the parameters which determine the photosynthesis-temperature response across broad plant functional types, it is reasonable in the model tuning process to adjust these parameters as a means of improving simulation of equilibrium vegetation distributions. The results of this study clearly indicate that adjusting temperature-photosynthesis parameters has strong implications for the transient response of the carbon cycle to climate warming, and as such, modelers should be aware of the potentially large effect that model tuning of this nature will have for the behavior of future carbon cycle-climate feedbacks. Furthermore, given that most land models share similar parameterizations of the photosynthesis-temperature response curve [*Friedlingstein et al.*, 2006], the sensitivity of carbon cycle-climate feedbacks to temperature control parameters shown here is generally applicable to all such models.

[43] As shown in section 3.2, the effect of temperature stress on photosynthesis is particularly evident in tropical areas. As such, the large carbon cycle-climate feedbacks in ALL and DT were driven largely by changes in tropical productivity. This result is relevant to recent studies from other modeling groups, notably results using the Hadley Centre's HadCM3LC model [*Cox et al.*, 2000; *Jones et al.*, 2003b]. A striking feature of the HadCM3LC runs was a large decrease in terrestrial carbon storage in the tropics as a result of climate changes; it is likely that this result was driven in large measure by high temperatures and decreased moisture availability, both of which decreased tropical primary productivity and amplified the overall climate feedback from the terrestrial biosphere [*Cox et al.*, 2001]. It is also notable that other models have not shown similar decreases in tropical terrestrial carbon storage. Both *Govindasamy et al.* [2005] and *Fung et al.* [2005] found increased tropical terrestrial carbon sinks in the INCCA and NCAR-CSM1 models, respectively, along with correspondingly small terrestrial carbon cycle feedbacks to climate. The UVic model results presented here demonstrate that tropical productivity responses to climate changes are critical in determining the overall strength of terrestrial carbon cycle-climate feedbacks, and we argue that this conclusion can be directly applied to results from other coupled climate-carbon models.

5. Conclusions

[44] This study highlights the sensitivity of the climate-carbon system to the choice vegetation parameters in coupled climate-carbon models. Both the simulated pre-industrial vegetation distribution and the transient response of the terrestrial carbon cycle to climate and CO_2 changes reflect any changes that are made to the parameterization of the terrestrial biosphere. The future strength of carbon cycle-climate feedbacks is very sensitive to model parameters, particularly if those parameter changes modify the impact of future climate changes on terrestrial productivity. This was demonstrated here most clearly in the case of temperature constraints on photosynthesis; however, different climate models could simulate different changes in environmental constraints on photosynthesis than those highlighted here. For example, pronounced continental drying as a result of atmospheric circulation changes would have a large impact on terrestrial carbon uptake, and contribute to a large amplification of the simulated future carbon cycle-climate feedback.

[45] It is possible that we are now beginning to see observational evidence of a potentially large terrestrial productivity contribution to carbon cycle-climate feedbacks. A recent analysis of terrestrial carbon dynamics during the 2003 summer heat-wave in Europe found that the combination of drought and high temperatures actually led the terrestrial biosphere to become a source for carbon due to a pronounced suppression of terrestrial photosynthesis [*Ciais et al.*, 2005]. It is conceivable that more such events in the future will further emphasize the critical role that terrestrial productivity plays in determining the net fluxes of carbon between the atmosphere and the land biosphere. On the basis of the results of our research, we argue that the future behavior of terrestrial productivity will be of first-order importance in determining the overall strength of future carbon cycle-climate feedbacks, and may in fact exceed the importance of the soil respiration-temperature response in explaining the very large range of feedbacks produced by different coupled climate-carbon models. It is clear that further research is required to better constrain future carbon cycle-climate feedbacks, both with respect to our understanding of how vegetation responds to changes in climatic constraints, and also in our ability to represent these processes in the current generation of global models.

[46] **Acknowledgments.** We would like to thank A. Weaver, S. Marshall, S. Sitch, and one anonymous reviewer for their advice and helpful comments on earlier versions of this manuscript. Funding support

from the National Science and Engineering Research Council of Canada and the Alberta Ingenuity Fund is gratefully acknowledged.

References

Adams, B., A. White, and T. M. Lenton (2004), An analysis of some diverse approaches to modelling terrestrial net primary productivity, *Ecol. Modell.*, *177*, 353–391.

Aerts, R. (2006), The freezer defrosting: Global warming and litter decomposition rates in cold biomes, *J. Ecol.*, *94*, 713–724.

Berry, J., and O. Björkman (1980), Photosynthetic response and adaptation to temperature in higher plants, *Annu. Rev. Plant Physiol.*, *31*, 491–543.

Ciais, P., et al. (2005), Europe-wide reduction in primary productivity caused by the heat and drought in 2003, *Nature*, *437*, 529–533.

Collatz, G. J., J. T. Ball, C. Grivet, and J. A. Berry (1991), Physiological and environmental regulation of stomatal conductance, photosynthesis and transpiration, *Agric. For. Meteorol.*, *54*, 107–136.

Collatz, G. J., M. Ribas-Carbo, and J. A. Berry (1992), A coupled photosynthesis-stomatal conductance model for leaves of C4 plants, *Aust. J. Plant Physiol.*, *19*, 519–538.

Cox, P. M. (2001), Description of the TRIFFID Dynamic Global Vegetation Model, *Tech. Note 24*, Hadley Cent., Met Office, Bracknell, U. K.

Cox, P. M., R. A. Betts, C. B. Bunton, R. L. H. Essery, P. R. Rowntree, and J. Smith (1999), The impact of new land surface physics on the GCM simulation of climate and climate sensitivity, *Clim. Dyn.*, *15*, 183–203.

Cox, P. M., R. A. Betts, C. D. Jones, S. A. Spall, and I. J. Totterdell (2000), Acceleration of global warming due to carbon-cycle feedbacks in a coupled climate model, *Nature*, *408*, 184–187.

Cox, P. M., R. A. Betts, C. D. Jones, S. A. Spall, and I. J. Totterdell (2001), Modelling vegetation and the carbon cycle as interactive elements of the climate system, *Tech. Note 23*, Hadley Cent., Met Office, Bracknell, U. K.

Dufresne, J.-L., P. Friedlingstein, M. Berthelot, L. Bopp, P. Ciais, L. Fairhead, H. Le Treut, and P. Monfray (2002), On the magnitude of positive feedback between future climate change and the carbon cycle, *Geophys. Res. Lett.*, *29*(10),1405, doi:10.1029/2001GL013777.

Essery, R. L. H., M. J. Best, R. A. Betts, P. M. Cox, and C. M. Taylor (2003), Explicit representation of subgrid heterogeneity in a GCM land surface scheme, *J. Hydrometeorol.*, *4*, 530–543.

Ewen, T. L., A. J. Weaver, and M. Eby (2004), Sensitivity of the inorganic ocean carbon cycle to future climate warming in the UVic coupled model, *Atmos. Ocean*, *42*, 23–42.

Friedlingstein, P., L. Bopp, P. Ciais, J.-L. Dufresne, L. Fairhead, H. Le Treut, P. Monfray, and J. Orr (2001), Positive feedback between future climate change and the carbon cycle, *Geophys. Res. Lett.*, *28*, 1543–1546.

Friedlingstein, P., J.-L. Dufresne, P. M. Cox, and P. Rayner (2003), How positive is the feedback between future climate change and the carbon cycle?, *Tellus, Ser. B*, *55*, 692–700.

Friedlingstein, P., et al. (2006), Climate-carbon cycle feedback analysis, results from the C4MIP model intercomparison, *J. Clim.*, *19*, 3337–3353.

Fung, I. Y., S. C. Doney, K. Lindsay, and J. John (2005), Evolution of carbon sinks in a changing climate, *Proc. Natl. Acad. Sci. U. S. A.*, *102*, 11,201–11,206.

Govindasamy, B., S. Thompson, A. Mirin, M. Wickett, K. Caldeira, C. Delire, and P. B. Duffy (2005), Increase of carbon cycle feedback with climate sensitivity: Results from a coupled climate and carbon cycle model, *Tellus, Ser. B*, *57*, 153–163.

Houghton, R. (2003), Revised estimates of the annual net flux of carbon to the atmosphere from changes in land use and land management 1850–2000, *Tellus, Ser. B*, *55*, 378–390.

Hungate, B. A., J. S. Dukes, M. R. Shaw, Y. Luo, and C. B. Field (2003), Nitrogen and climate change, *Science*, *302*, 1512–1513.

Jones, C. D., P. Cox, and C. Huntingford (2003a), Uncertainty in climate-carbon cycle projections assiciated with the sensitivity of soil respiration to temperature, *Tellus, Ser. B*, *55*, 642–648.

Jones, C. D., P. M. Cox, R. L. H. Essery, D. L. Roberts, and M. J. Woodage (2003b), Strong carbon cycle feedbacks in a climate model with interactive CO_2 and sulphate aerosols, *Geophys. Res. Lett.*, *30*(9), 1479, doi:10.1029/2003GL016867.

Jones, C., C. McConnell, K. Coleman, P. Cox, P. Falloon, D. Jenkinson, and D. Powlson (2005), Global climate change and soil carbon stocks: Predictions from two contrasting models for the turnover of organic carbon in soil, *Global Change Biol.*, *11*, 154–166.

Kirschbaum, M. U. F. (2004), Direct and indirect climate change effects on photosynthesis and transpiration, *Plant Biol.*, *6*, 242–253.

Lambers, H., F. S. Chapin III, and T. L. Pons (1998), *Plant Physiological Ecology*, 540 pp., Springer, New York.

Loveland, T., and A. Belward (1997), The IGBP-DIS global 1 km land cover data set, DISCover: First results, *Int. J. Remote Sens.*, *18*, 3289–3295.

Marland, G., T. A. Boden, and R. J. Andres (2002), Global, regional, and national annual CO_2 emissions from fossil-fuel burning, cement production, and gas flaring: 1751-2000, in *CDIAC NDP-030*, http://cdiac.esd.ornl.gov/trends/trends.htm, Carbon Dioxide Inf. Anal. Cent., Oak Ridge Natl. Lab., Oak Ridge, Tenn.

Matthews, H. D., M. Eby, A. J. Weaver, and B. J. Hawkins (2005a), Primary productivity control of simulated carbon cycle-climate feedbacks, *Geophys. Res. Lett.*, *32*, L14708, doi:10.1029/2005GL022941.

Matthews, H. D., A. J. Weaver, and K. J. Meissner (2005b), Terrestrial carbon cycle dynamics under recent and future climate change, *J. Clim.*, *18*, 1609–1628.

Medlyn, B. E., D. Loustau, and S. Delzon (2002a), Temperature response of parameters of a biochemically based model of photosynthesis. I. Seasonal changes in mature maritime pine (Pinus pinaster Ait.), *Plant Cell Environ.*, *25*, 1155–1165.

Medlyn, B. E., et al. (2002b), Temperature response of parameters of a biochemically based model of photosynthesis. II. A review of experimental data, *Plant Cell Environ.*, *25*, 1167–1179.

Meissner, K. J., A. J. Weaver, H. D. Matthews, and P. M. Cox (2003), The role of land-surface dynamics in glacial inception: a study with the UVic Earth System Climate Model, *Clim. Dyn.*, *21*, 515–537.

Nakićenović, N., et al. (2000), *Special Report on Emissions Scenarios*, 570 pp., Cambridge Univ. Press, New York.

Prentice, C., et al. (2001), The carbon cycle and atmospheric carbon dioxide, in *Climate Change 2001: The Scientific Basis*, edited by J. T. Houghton et al., pp. 183–237, Cambridge Univ. Press, New York.

Reich, P. B., M. B. Walters, and D. S. Ellsworth (1997), From tropics to tundra: Global convergence in plant functioning, *Proc. Natl. Acad. Sci. U. S. A.*, *94*, 13,730–13,734.

Reich, P. B., D. S. Ellsworth, M. B. Walters, J. M. Vose, C. Gresham, J. C. Volin, and W. D. Bowman (1999), Generality of leaf trait relationships: A test across six biomes, *Ecology*, *80*, 1955–1969.

Saugier, B., J. Roy, and H. A. Mooney (2001), Estimations of global terrestrial productivity: Converging toward a single number?, in *Terrestrial Global Productivity: Past Present and Future*, edited by J. Roy, B. Saugier, and H. Mooney, pp. 543–557, Elsevier, New York.

Schäfer, K. V. R., et al. (2002), Hydrologic balance in an intact temperate forest ecosystem under ambient and elevated atmospheric CO_2 concentration, *Global Change Biol.*, *8*, 895–911.

Thompson, S. L., B. Govindasamy, A. Mirin, K. Caldeira, C. Delire, J. Milovich, M. Wickett, and D. Erickson (2004), Quantifying the effects of CO_2-fertilized vegetation on future global climate and carbon dynamics, *Geophys. Res. Lett.*, *31*, L23211, doi:10.1029/2004GL021239.

Weaver, A. J., et al. (2001), The UVic Earth System Climate Model: Model description, climatology and applications to past, present and future climates, *Atmos. Ocean*, *39*, 361–428.

Wright, I. J., et al. (2004), The worldwide leaf economics spectrum, *Nature*, *428*, 821–827.

Zeng, N., H. Qian, and E. Munoz (2004), How strong is carbon cycle-climate feedback under global warming?, *Geophys. Res. Lett.*, *31*, L20203, doi:10.1029/2004GL020904.

M. Eby, School of Earth and Ocean Sciences, University of Victoria, P.O. Box 3055, Stn CSC, Victoria, BC, Canada V8W 3P6. (eby@uvic.ca)

T. Ewen, Institute for Atmospheric and Climate Science, ETH Zurich, Universitatstrasse 16, CH-8092 Zurich, Switzerland. (tracy.ewen@env.ethz.ch)

P. Friedlingstein, Institute Pierre Simon Laplace, LSCE, L'Orme des Merisiers, Bat 712, Gif sur Yvette, F-91191 France. (pierre.friedlingstein@cea.fr)

B. J. Hawkins, Centre for Forest Biology, University of Victoria, P.O. Box 3055, Stn CSC, Victoria, BC, Canada V8W 3P6. (bhawkins@uvic.ca)

H. D. Matthews, Department of Geography, Planning and Environment, Concordia University, 1455 de Maisonneuve Blvd W, Montreal, QC, Canada H3G 1M8. (dmatthew@alcor.concordia.ca)